RSC Advances

PAPER

View Article Online
View Journal | View Issue

Cite this: *RSC Adv.*, 2021, **11**, 5938

Synthesis and solvent-controlled self-assembly of diketopiperazine-based polyamides from aspartame†

Hongrong Yin, [a] Kenji Takada, [a] Amit Kumar, [a] Thawinda Hirayama[b] and Tatsuo Kaneko *[a]

An aspartame-based AB-type diketopiperazine monomer, cyclo(L-aspartyl-4-amino-L-phenylalanyl) (ADKP), was synthesized and subsequently utilized in the polycondensation of homo-polyamides with high molecular weights. By using various amino acids, dicarboxylic acids, and diamines, random DKP-based copolymers were also synthesized. The self-assembly properties of ADKP and poly(cyclo(L-aspartyl-4-amino-L-phenylalanyl)) (PA1) were studied *via* the solvent displacement method. Notably, PA1 self-assembled into particles with various morphologies in different solvent systems, such as irregular networks, ellipsoids, and hollow particles. The morphological transformation was also confirmed by dropping acetone and toluene onto the PA1 particles. Furthermore, infrared spectra and Hansen solubility parameters of PA1 and different solvents revealed the particle formation mechanism, which provided more insights into the relationship between the morphology and strength of the hydrogen bonding of each solvent.

Received 30th November 2020
Accepted 28th January 2021

DOI: 10.1039/d0ra10086b

rsc.li/rsc-advances

Introduction

Amino acids are important renewable resources for food, medical, and biological studies, as well as synthetic materials.[1–5] Amino acids and their derivatives have been used as monomers for functional and high-performance polymers.[6–8] Notably, 2,5-diketopiperazines (DKPs), which are cyclic α-amino acid dimers, contain two centrosymmetric s-*cis*-amide bonds in a six-membered ring. DKPs have multiple hydrogen bonding acceptor and donor sites in a rigid ring, which enable the formation of regular molecular assembly through continuous intermolecular hydrogen bonding.[9–12] This remarkable DKP self-assembly behavior has been attracting the attention of scientists in crystal engineering, gelators, and supramolecular architectures.[13–19] As described above, DKPs exhibit a unique particle morphology, even when they are used as monomers; it can be expected that they still exhibit such morphologies when they adopt a polymer structure. In addition, the rigid structure of DKP may impart high thermal and mechanical properties to polymeric materials.[20,21] The continuous hydrogen bonding of DKP units in polymer chains may lead to unique self-assembly.[22] However, only a few DKP-based polymers have been reported, and their self-assembly properties have not been adequately studied.[20–24] The main problem in the development of DKP-based polymers is the low solubility, which induces lower molecular weight and complicates property evaluation. Thus, the design of DKP monomers with high solubility is important for obtaining self-assembled DKP polymers. Almost all DKP monomers used in the literature have been obtained from the homo-coupling of amino acids, which exhibit high symmetry and tend to increase the crystallinity and decrease the solubility in many solvents. The use of asymmetric AB-type monomers of two different amino acids is envisaged to be one of the efficient methods to control solubility.[16,25,26] Masuda *et al.* reported various synthesis approaches of DKP-based polymers and confirmed that the hydrogen bonding of DKP moieties affected polymer properties.[23] We recently reported DKP-based polyimides whose particles showed high heat resistance and polymorphism properties.[24] However, the self-assembly mechanism of the DKP moiety in polymers remains unclear, while self-assembly is a bottom-up formation of ordered structures under thermodynamic and kinetic conditions.[5,27–30] The self-assembly behavior of DKPs with low molecular weight has been reported to be deeply affected by conditions and environment. In a solution system, DKP–DKP interactions always compete with DKP-solvent interactions; therefore, investigating the interaction nature of both DKP-based polymers and solvents is important.[31,32]

[a]*Energy and Environment Area, Japan Advanced Institute of Science and Technology, 1-1 Asahidai, Nomi, Ishikawa 923-1292, Japan. E-mail: kaneko@jaist.ac.jp*

[b]*Department of Chemistry, Faculty of Science, Chulalongkorn University, 254 Phayathai Road, Pathumwan, Bangkok 10330, Thailand*

† Electronic supplementary information (ESI) available: ^{1}H NMR spectra, ^{13}C NMR spectrum and FTIR spectra of obtained monomer. ^{1}H NMR spectrum, FTIR spectrum, TGA curves XRD spectrum and table of solubilities of PA1 or PAs. See DOI: 10.1039/d0ra10086b

The L-aspartyl-L-phenylalanine methyl ester is a synthetic sweetener that is commercially known as aspartame; it is one of the most highly produced peptides worldwide.[33,34] Further, it is known that intramolecular cyclocondensation of aspartame occurs through heating, and aspartame diketopiperazine (APM-DKP) with an asymmetric structure is produced.[35,36] Therefore, aspartame can be a promising candidate for synthesizing the above-mentioned highly soluble DKP and its polymer.

The present article deals with the synthesis of an AB-type DKP with high solubility using a simple and commercially available method. The obtained DKP monomer was applied to the polymerization reactions of polyamides with or without using other monomers. Moreover, the morphological control and self-assembly mechanism of DKP-based polyamides were investigated.

Experimental section

Material

L-Aspartyl-L-phenylalanine methyl ester was supplied by Ajinomoto Co., Inc. Triphenyl phosphite ($P(OPh)_3$), L-phenylalanine (Phe), succinic acid, ethylene diamine and *p*-phenylenediamine were purchased from Tokyo Chemical Industry Co., Ltd. 5% Palladium on activated carbon (Pd/C) and *N*-methylpyrrolidone (NMP) were purchased from FUJIFILM Wako Pure Chemical Corporation. Dimethyl sulfoxide (DMSO), sulfuric acid, nitric acid, pyridine, ethanol, tetrahydrofuran, ethyl acetate, acetone and toluene were purchased from Kanto Chemical Co., Inc. All the chemicals were directly used as purchased.

Measurements

^{1}H NMR and ^{13}C NMR spectra were performed by a Bruker Biospin AG 400 MHz, 54 mm spectrometer using DMSO-d_6 as the solvent. The FT-IR spectra were recorded with a Perkin-Elmer Spectrum One spectrometer between 4000 and 400 cm^{-1} using a diamond-attenuated total reflection (ATR) accessory. The mass spectra were measured using a FT-ICR MS (Solarix) equipped with a Nanospray source operating in the nebulizer-assisted ESI mode used in the negative ion mode and scanned from m/z 50 to m/z 1000. The number-average molecular weight (M_n), weight-average molecular weight (M_w) and the molecular weight distribution (M_w/M_n) were determined by gel permeation chromatography (GPC, concentration 1 g L^{-1}, 10 mM LiBr/DMF eluent) after calibration with polystyrene standards using two of OHpack SB-806M HQ column (Shodex). Thermogravimetric analysis (TGA) and differential scanning calorimetry (DSC) were carried out by Seiko Instruments SII, SSC/5200 and Seiko Instruments SII, X-DSC7000T, respectively, at a heating rate of 5 °C min^{-1} under a nitrogen atmosphere. Remaining solvent and absorbed moisture in polymer samples were removed at 200 °C for 1 hour before TGA and DSC measurement. Monomer and polymer particles morphology were characterized with scanning electron microscope (JCM-6000Plus Versatile Benchtop SEM). Samples were coated with a layer of gold in thickness of 15 nm by a sputter coater (Magnetron sputter MSP-1S). SEM instrument was operated at an acceleration voltage of 10 kV and an emission current of 10 μA. Hansen solubility parameters of polymer and solvents are calculated by Hansen Solubility Parameters in Practice (HSPiP) 5th Edition software.

Synthesis of cyclo(L-aspartyl-L-phenylalanyl) (AMP–DKP)

L-Aspartyl-L-phenylalanine methyl ester (5.86 g, 20.0 mmol) was dissolved in DMSO (20 mL) and stirred at 80 °C for 8 h. The resulting solution was added into a mixture of acetone (300 mL) and hexane (300 mL) to obtain a precipitate. The white precipitate was obtained by filtration and dried in a vacuum oven at 100 °C with a yield of 4.61 g (88%).

Synthesis of cyclo(L-aspartyl-4-nitro-L-phenylalanyl) (NDKP)

Here, APM-DKP (1.30 g, 4.96 mmol) was dissolved in concentrated sulfuric acid (30 mL) in an ice bath. A prepared solution mixture of nitric acid (1 mL) and sulfuric acid (4 mL) was added dropwise to the APM-DKP sulfuric acid solution at 0 °C. Subsequently, the solution was stirred for 5 min. The resulting solution was poured into ice water (300 mL) dropwise and the pH was adjusted to approximately 5 by adding sodium hydroxide solution. Thereafter, the solution was extracted with ethyl acetate (200 mL) three times and vapor was removed using a vacuum evaporator and vacuum oven at 100 °C. The objective product was obtained as a white powder with a 73% yield(1.10 g). ^{1}H NMR (400 MHz, DMSO-d_6, δ, ppm): 2.07 (dd, 1H, J = 5.9, 16.6 Hz), 2.28 (dd, 1H, J = 5.4, 16.6 Hz), 3.10 (dd, 1H, J = 5.3, 14.0 Hz), 3.24 (dd, 1H, J = 4.8, 13.9 Hz), 4.11 (t, 1H, J = 5.6 Hz), 4.34 (t, 1H, J = 5.1 Hz), 7.49 (d, 2H, J = 8.7 Hz), 8.1 (s, 1H), 8.17 (d, 1H, J = 8.7 Hz), 8.23 (s, 1H).

Synthesis of cyclo(L-aspartyl-4-amino-L-phenylalanyl) (ADKP)

NDKP (0.50 g, 1.63 mmol) not subjected to purification was dissolved in pure water, and Pd/C (0.11 g, 22 wt%) was added. The mixture was connected with a hydrogen generator and reacted with hydrogen at a feed rate of 500 mL min^{-1} at 50 °C for 6 h. The resulting mixture was filtered and evaporated under vacuum. The resulting solid was recrystallized in water and dried in a vacuum oven at 100 °C with an 88% yield (0.40 g). ^{1}H NMR (400 MHz, DMSO-d_6, δ, ppm): 1.63 (dd, 1H, J = 7.4, 11.9 Hz), 2.12 (dd, 1H, J = 5.1, 16.4 Hz), 2.72 (dd, 1H, J = 4.6, 13.8 Hz), 2.91 (dd, 1H, J = 4.2, 13.7 Hz), 4.01 (t, 1H, J = 6.0 Hz), 4.05 (t, 1H, J = 4.7 Hz), 6.46 (d, 2H, J = 8.3 Hz), 6.80 (d, 2H, J = 8.3 Hz), 7.83 (s, 1H), 7.98 (s, 1H). FT-ICR MS (ESI): calcd for $[C_{13}H_{14}N_3O_4]^-$, 276.10626, found 276.09867.

Syntheses of ADKP-based polyamides (PAs)

A typical polymerization procedure for DKP-based polyamides is shown below. ADKP (0.055 g, 0.2 mmol) was mixed with $P(OPh)_3$ (40 μL, 0.15 mmol), pyridine (50 μL, 0.6 mmol), and NMP (100 μL). The reaction solution was stirred at 100 °C for 48 h under nitrogen atmosphere. After the reaction finished, the resulting solution was precipitated in acetone, and the resulting solid was washed with acetone and dried in a vacuum oven at 100 °C to give PA1 as a yellow powder with an 84% yield.

Following the same protocol, ADKP (0.027 g, 0.1 mmol) was treated with other monomers such as L-phenylalanine (0.016 g, 0.1 mmol) to synthesize PA2 with a 79% yield; further, succinic acid (0.012 g, 0.1 mmol) was treated with ethylene diamine (67 μL, 0.1 mmol) to synthesize PA3 with a 81% yield, and succinic acid (0.012 g, 0.1 mmol) was treated with *p*-phenylenediamine (0.011 g, 0.1 mmol) to synthesize PA4 with a 84% yield.

Preparation of particles of ADKP and ADKP-based polyamides

The obtained ADKP or PA1 (*ca.* 2.5 mg) were dissolved in 1 mL DMSO as a stock solution. Next, a 0.1 mL stock solution was dispersed into 3 mL of different poor solvents, such as water, ethanol, THF, ethyl acetate, acetone, and toluene, under vigorous magnetic stirring. A droplet (3 μL) of the dispersion liquid was dropped on a glass slide and air-dried to assess the SEM images.

In the secondary solvent treatment route 1, 0.1 mL PA1 stock solution was dispersed into 3 mL of toluene under stirring. A droplet (3 μL) of the dispersion liquid was dropped on a glass slide and dried. After drying, a droplet (3 μL) of acetone was dropped on the sample glass slide and dried for the SEM observation. In route 2, similarly, 0.1 mL PA1 stock solution was dispersed into 3 mL of acetone under stirring. A droplet (3 μL) of the dispersion liquid was dropped on a glass slide and dried. After drying, a droplet (3 μL) of toluene was dropped on the sample glass slide and dried for the SEM observation. In route 3, 0.1 mL PA1 stock solution was dispersed into 3 mL of acetone under stirring. A droplet (3 μL) of the dispersion liquid was dropped on a glass slide and a droplet (3 μL) of toluene was added immediately. After drying, a part of the sample was observed by SEM. And a droplet (3 μL) of acetone was dropped on another part of sample and dried for SEM observation.

The drying process of all samples was under air humidity of about 40–45% and temperature of 25 °C.

Results and discussion

Monomer syntheses

The solubility of DKP derivatives is low due to the rigid six-membered ring and the strong intermolecular hydrogen bond, although monomer solubility is a key factor for efficient polymerization. Almost all of the reported AA-type DKP monomers exhibiting low solubility were converted into polymers with low molecular weights and poor performances. To solve this problem, we designed a new AB-type DKP monomer that was expected to demonstrate high solubility. The AB-type DKP-based monomer ADKP was obtained from the L-aspartyl-L-phenylalanine methyl ester, following intramolecular condensation, nitration, and reduction (Scheme 1). Notably, after the nitration of APM-DKP, both *para*-substituted and *ortho*-substituted products were confirmed (Fig. S1†). The ratio of the *para*-substituted product to the *ortho*-substituted product was 9 : 1, as calculated by NMR. Recrystallization of the crude product could not completely remove the *ortho*-substituted product. However, the reduction product could be easily recrystallized to give pure *para*-substituted ADKP. The structure of ADKP was confirmed by ^{1}H NMR, ^{13}C NMR, FTIR and ESI-MS (Fig. S1–S3†).

As a result, the obtained ADKP showed high solubility in water and polar organic solvents such as methanol, NMP, DMF, and DMSO (Table 1). The high solubility of ADKP is attributable to the asymmetric structure, which increases the solvation entropy of ADKP.[37] Otherwise, the existence of ionic amine and carboxylic groups can contribute to solubility, which disturbs the formation of intermolecular hydrogen bonds between the DKP moieties in solvated states.[38]

Polymer syntheses

PAs were prepared by homo-polymerization or co-polymerization of ADKP as an AB-type monomer (with or without other comonomers) using $P(OPh)_3$ and pyridine as condensation reagents (Scheme 2). ^{1}H NMR spectra of the obtained PAs showed a new peak at 9.5 ppm due to the phenyl amide proton, and amide protons in the DKP moiety remained unchanged at 7.9 and 8.1 ppm which confirmed the presence of the ADKP moiety in all PAs, including co-polymers PA2, PA3 and PA4 (see Fig. S4†). In addition, the M_w and M_n of PAs have been determined by GPC (Fig. S5†), which are summarized in Table 2. Based on these results, the polymerizations of ADKP successfully proceeded, and the molecular weights were

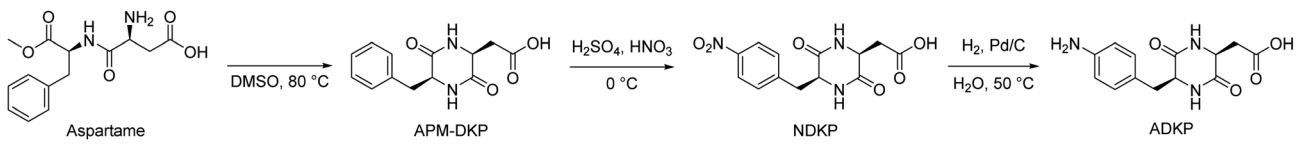

Scheme 1 Synthesis of AB-type DKP-based monomer from aspartame.

Table 1 Solubility of NDKP and ADKP[a]

	Water	Methanol	Ethanol	Acetone	DMSO	DMF	DMAc	NMP
NDKP	±	±	±	±	+	+	+	+
ADKP	+	+	+	±	+	+	+	+

[a] Conditions; samples, 10 mg; solvent, 2 mL; temperature, r.t.; (+), soluble; (±), partially soluble; (−), insoluble.

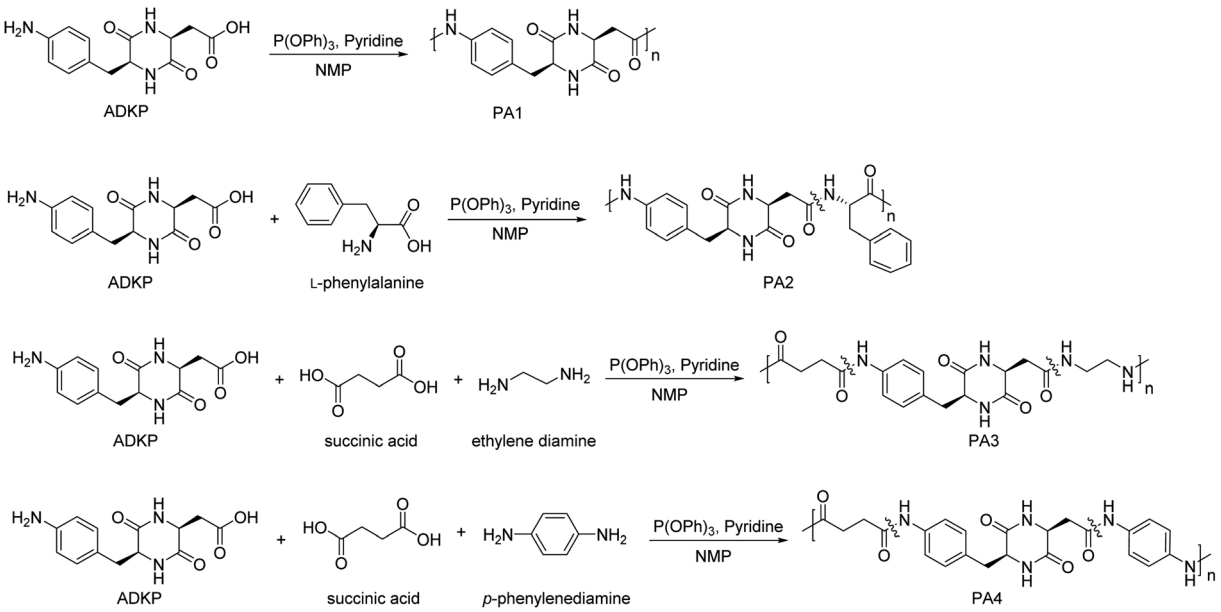

Scheme 2 Synthesis of DKP-based polyamides from cyclo(L-aspartyl-4-amino-L-phenylalanyl).

observed to be in the range of 1.59–1.98 $\times$ 10^4 g mol^{-1}; the M_w/M_n ratio was 1.17–1.36. Moreover, all the GPC traces showed monomodal distribution. These results supported that co-polymerizations were progressed. Furthermore, the obtained PAs are soluble in NMP, DMSO, DMAc, and concentrated sulfuric acid (Table S1†). The high molecular weight of PAs is due to the high solubility of the monomers and polymers in organic solvents.

Thermal properties of PAs

TGA was utilized to evaluate the thermal decomposition of PAs in a nitrogen atmosphere. As shown in Table 2 and Fig. S6,† the 5% and 10% weight-loss temperatures (T_{d5} and T_{d10}) of PAs ranged from 272–326 °C. Remarkably, although all PAs had similar molecular weights, the homopolymer PA1 revealed the highest T_{d5} and T_{d10} values, which was approximately 50 °C higher than the others. Moreover, the thermal physical transformation of PAs was investigated *via* DSC in a nitrogen atmosphere. However, between 50 °C and 250 °C, no glass transition temperature (T_g), melting temperature (T_m), or recrystallization temperature was detected. These results indicate that PA1 has the simplest chemical structure among all PAs, with the most abundant DKP moiety and benzene ring, which is considered to contribute to its relatively superior thermal properties.

Self-assembly behaviors of DKP-based monomer and PA1

DKP derivatives with low molecular weights are well known for their orderly aggregation through parallel hydrogen bonds, which are utilized to fabricate crystals or semi-crystals with various morphologies. Long chains reduce the crystallinity of polymeric systems,[39] which may lead to different self-assembling behaviors that originate from small DKP derivatives. In this study, the simple DKP-based polymer (PA1) was considered a suitable model for carrying out the self-assembly study; subsequently, it was used for particle fabrication. The solvent displacement method was adopted for the self-assembly studies of ADKP and PA1. Firstly, using ADKP as a monomer, the particle was prepared as follows: a DMSO solution of ADKP was slowly dropped into toluene to rapidly form particles. Furthermore, SEM images revealed the flower-like morphology of the particles (Fig. 1a). Flowers consist of two-dimensional petals with a soft and smooth surface. It is suggested that, with continuous hydrogen bonding between DKPs, ADKP may self-assemble into a planar tape-like structure, resulting in a petal-like substructure. As shown in Fig. 1b, all the petals were observed to bend inwards, and were suspended in toluene for 1 d. Therefore, petal bending can be regarded as a result of the reduction of surface free energies.[40] The same protocol was used for the self-assembly of PA1. To evaluate the effects of poor solvents on particulation, a DMSO solution of PA1 was dropped into water, ethanol, tetrahydrofuran, ethyl acetate, acetone, and toluene to precipitate particles. In cases of uses of water, ethanol, and THF, irregular network-like morphologies were observed (Fig. 1c–e). However, in ethyl acetate, ellipsoids were formed (Fig. 1f). In case of acetone and toluene, particles with hollow structures were observed (Fig. 1g and h). Notably, in contrast to other hollow particles reported in the literature,[41–44] the PA1 homopolymer (without any side chain and template) spontaneously self-assembled into a hollow morphology, which is a unique case for polymeric hollow particles. The particle sizes from acetone and toluene were approximately 1 μm and 12 μm, respectively. Because of the thin shell, these hollow particles show a porous structure or tend to collapse into a bow-like structure.

Table 2 Molecular weights and thermal properties of PAs derived from ADKP

Polymers	M_w[a] ($\times 10^4$ g mol^{-1})	M_n[a] ($\times 10^4$ g mol^{-1})	M_w/M_n[a]	T_{d5}[b] (°C)	T_{d10}[b] (°C)
PA1	1.93	1.64	1.18	326	348
PA2	1.59	1.36	1.17	276	296
PA3	1.76	1.36	1.29	272	289
PA4	1.98	1.46	1.36	280	302

[a] Determined by GPC measurements based on polystyrene standards; eluent, 10 mmol L^{-1} of LiBr DMF solution. [b] T_{d5} and T_{d10} were observed from TGA curve scanned at a heating rate of 5 °C min^{-1} under nitrogen atmosphere.

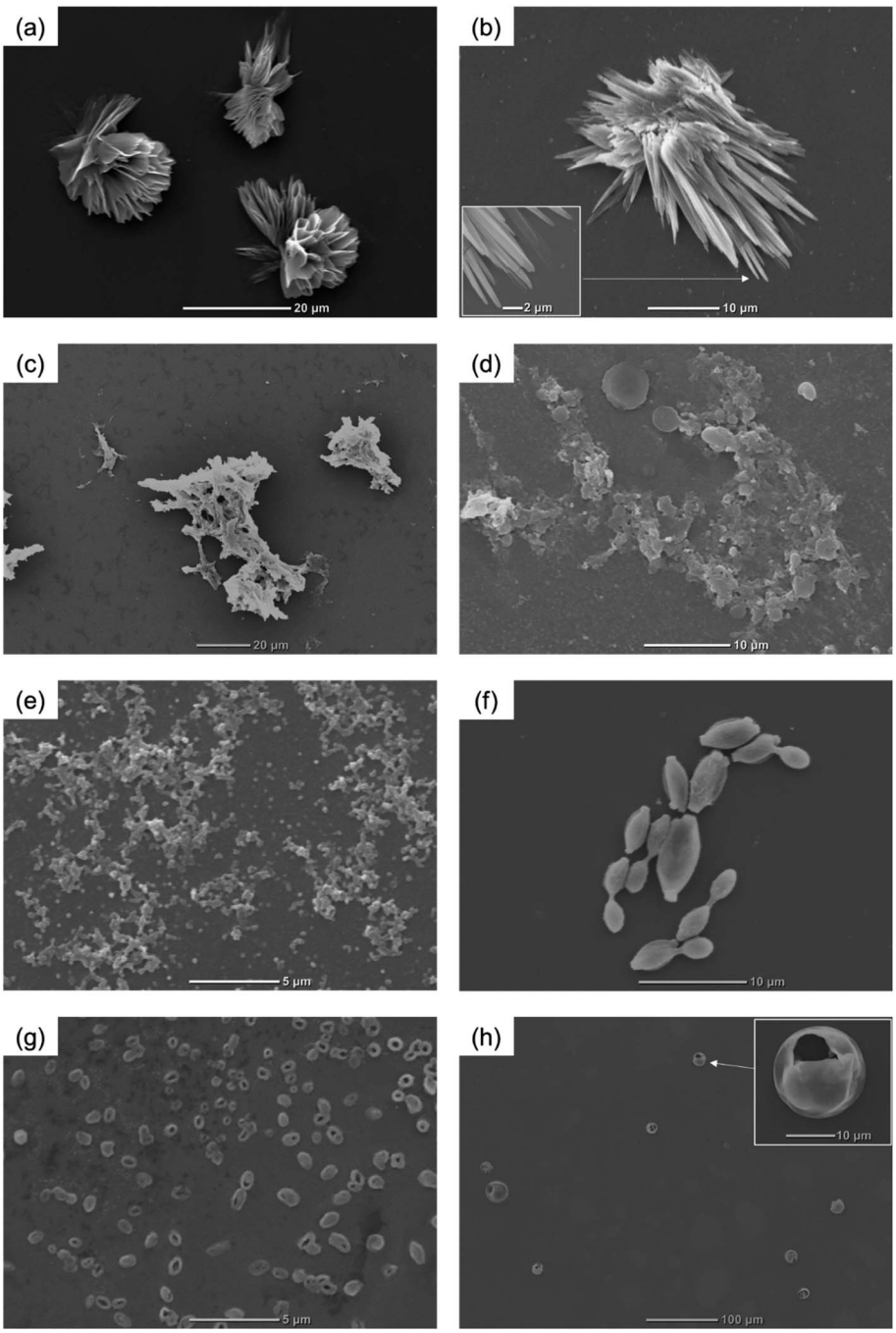

Fig. 1 SEM images of particles obtained by the dispersion of ADKP into toluene, (a) immediately after dispersion, (b) 1 d aging after dispersion, and PA1 into (c) water, (d) ethanol, (e) THF, (f) ethyl acetate, (g) acetone, and (h) toluene.

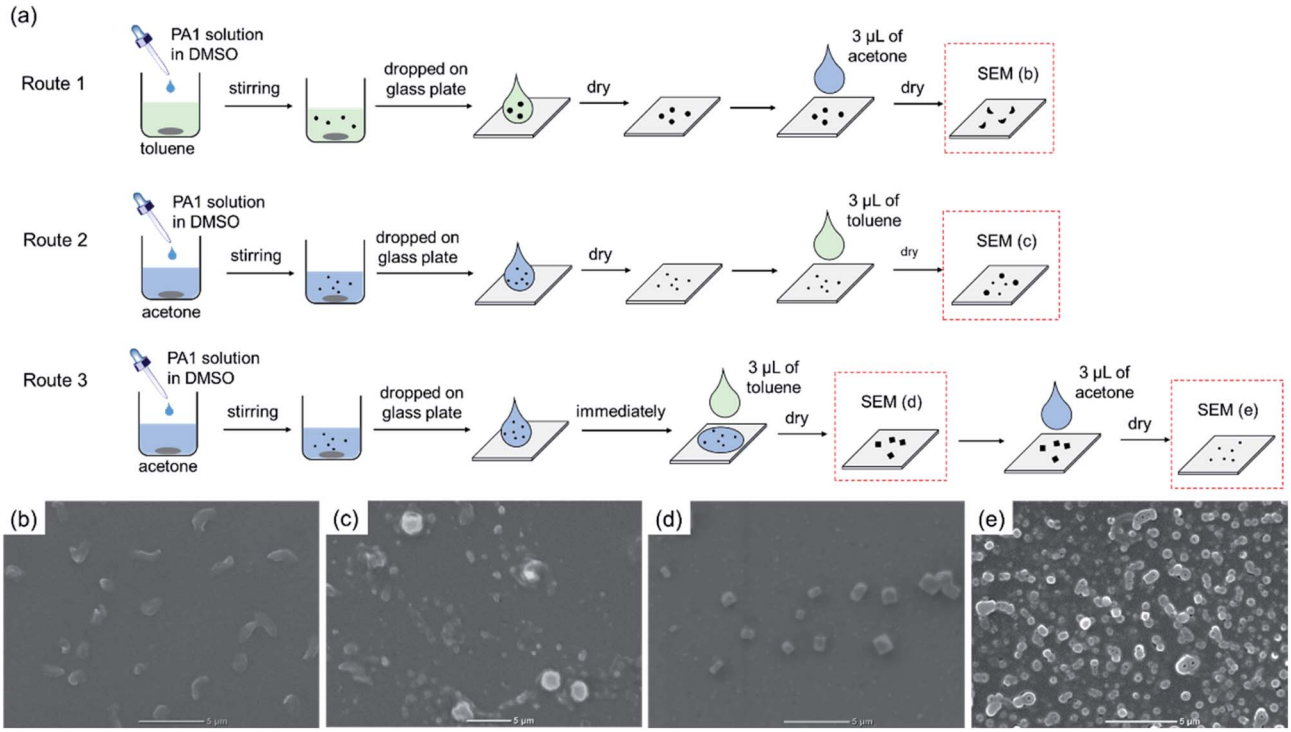

Fig. 2 (a) Process illustration of particle formation and transformation. SEM images of particles obtained in different processes related to the process illustration: particles obtained by (b) adding acetone into particles formed from toluene, (c) adding toluene into particles formed from acetone, (d) adding toluene into the suspension of the acetone sample, and (e) adding acetone into particles formed from mixture of acetone and toluene.

Morphology transformation

The self-assembly of PA1 was highly sensitive to the solvent environment as observed in the solvent displacement method, which provided primitive thermodynamic conditions. Notably, self-assembly is a thermodynamic process to reduce the free energies of the systems. Therefore, if the environment changes, a morphological transformation of PA1 particles may occur.[24] The morphological transformation was further investigated through the secondary solvent treatment of the formed particles. The treatment procedures are shown in Fig. 2a. By adding 3

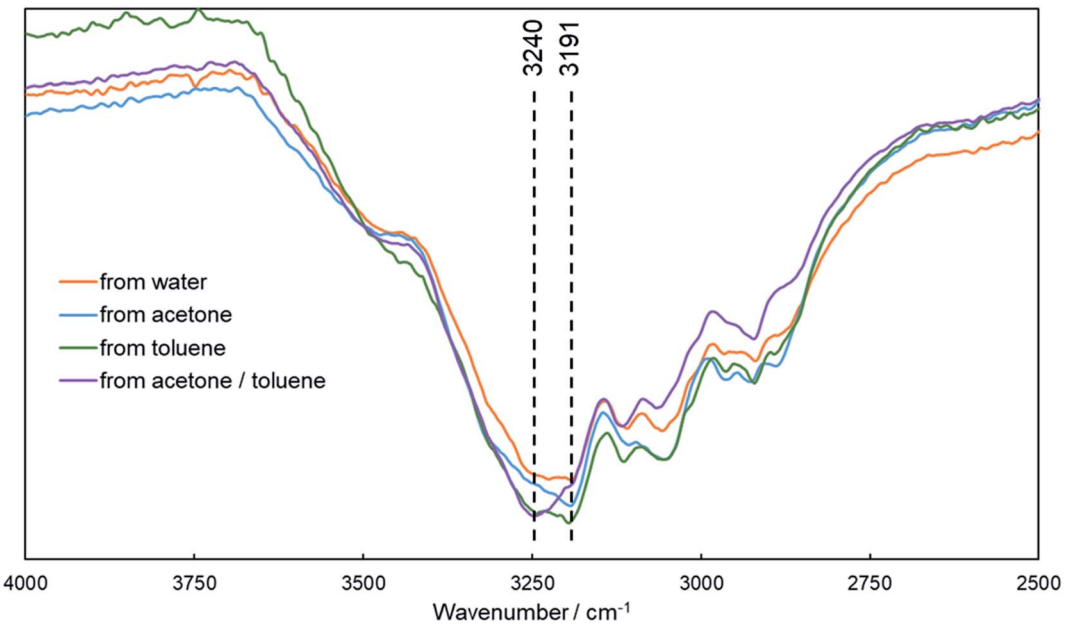

Fig. 3 IR spectra of PA1 particles precipitated from water, acetone, toluene, and mixture of acetone/toluene.

Table 3 Hansen solubility parameters of PA1 and solvents

Molecules	δ_D (MPa$^{0.5}$)	δ_P (MPa$^{0.5}$)	δ_H (MPa$^{0.5}$)
PA1	22.2	13.1	7.9
Water	15.5	16	42.3
Ethanol	15.8	8.8	19.4
Tetrahydrofuran	16.8	5.7	8
Ethyl acetate	15.8	5.3	7.2
Acetone	15.5	10.4	7
Toluene	18	1.4	2

μL acetone to the particles formed over toluene and subsequent drying in ambient air condition, hollow particles (same form of Fig. 1f) were broken into peel-like particles in the size of about 2 μm (route 1, Fig. 2b). Similarly, by simply changing the precipitate solvent to acetone and adding 3 μL toluene on the particles formed, after drying, small particles seemed to fuse into larger particles (route 2, Fig. 2c). Nonetheless, when toluene was added to the droplet of the acetone sample without drying, cubic particles were formed (route 3, Fig. 2d). Cubic particles are expected to have high crystallinity based on hydrogen bonds. However, X-ray diffraction did not show any distinct diffraction due to the small amount of cubic particles used for measurement (Fig. S7†). A similar behavior to cube formation has been previously reported for amphipathic polypeptides poly{γ-glutamic acid-*g*-(L-phenylalanine ethyl)}, but PA1 is not amphipathic.[45] However, both results indicated that molecular assembly through the π-stacking of phenylalanine moiety was important to form cubic morphology. In addition, based on such morphological changes that depend on the solvent, the addition of 3 μL acetone on the cubic particles after drying transformed the cubic particles into a spherical morphology that appeared porous or hollow (route 3, Fig. 2e). These hollow particles had a disordered shape because they were not vigorously stirred. Furthermore, it was envisaged that the shape would be the same as that shown in Fig. 1h, if the same experimental operation as that used for the particle preparation was performed.

Evaluation of the strength of hydrogen bond by FTIR spectroscopy

In the previous section, particle formations were dependent on the solvent, which in turn were dependent on the strength of the hydrogen bond for the solvent and PA.[46] Thus, the FTIR spectra were studied to evaluate the hydrogen bond behavior in the self-assembled particles formed in different solvents. Three types of morphologies were observed for the four solvents: irregular networks of water, hollow particles of acetone or toluene, and cubic particles of the solvent produced by mixing acetone and toluene. Fig. 3 shows the IR absorption in the N–H stretching vibration region. A shoulder peak for N–H stretching appears in all particles, whereby the band around 3191 cm^{-1} indicates a moderate hydrogen bond, and the band at 3240 cm^{-1} indicates the free N–H group.[47] In particles formed from water, the shoulder peak is flat, indicating that the number of free N–H and the hydrogen bond-interacted N–H was approximately equal. The distinct peak around 3191 cm^{-1} in the particles formed from acetone and toluene indicated the strong hydrogen bond, thereby suggesting a continuous hydrogen bond in the PA intra/inter molecules. Specifically, particles from toluene exhibits stronger peak at 3191 cm^{-1} and weaker peak at 3240 cm^{-1} compared to particles from acetone. It suggests that more and stronger hydrogen bonds were formed between DKP units in particles from toluene, which presumably affected the size of hollow spheres. On the other hand, for the particles formed from the solvent mixture of acetone and toluene, the bands at 3191 cm^{-1} and 3240 cm^{-1} became weaker and stronger, respectively. It is considered that acetone and toluene produce particles with strong hydrogen bonds, while their solvent mixture results in particles with weak hydrogen bonds. It is suspected that in particles that are formed from a mixed solvent, π-stacking becomes a dominant interaction rather than hydrogen bonding, thereby resulting in different morphologies.

Hansen solubility parameters

As discussed above, the self-assembly of PA1 was strongly affected by solvent composition. Solvent parameter evaluation has become a powerful tool to explain gelation, crystal growth, polymer aggregation, and other colloidal phenomena.[31,32,48,49] Here, we use Hansen solubility parameters (HSP), which include dispersion (δ_D), polarity (δ_P), and hydrogen bond (δ_H), to explain such a complicated polymorphism.[50,51] The HSPs of PA1 and the solvents used for elucidating the morphologies are summarized in Table 3. The δ_D and δ_P values for solvents seem to have little relation with particle morphology. Compared to

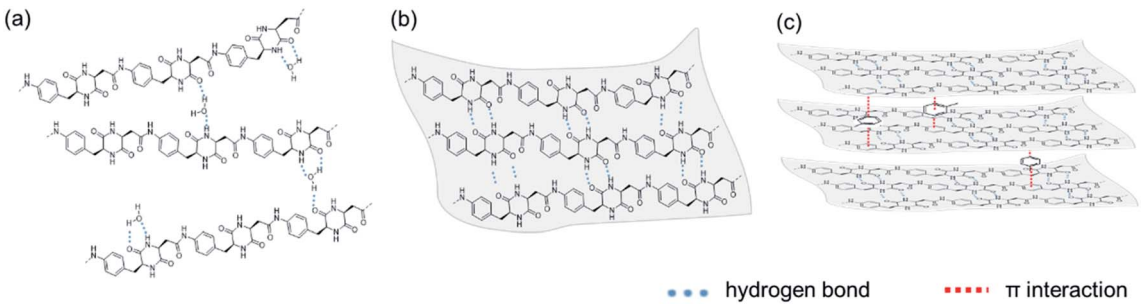

Fig. 4 Schematic illustration of formation of (a) irregular gel-like morphologies, (b) sheet-like substructure and (c) cubic particles.

the hydrogen bond, the dispersion interaction and dipole–dipole interaction are weak, which are considered to have less influence on the self-assembly of PA1 with multiple hydrogen bonding sites. As for δ_H, when solvents have higher δ_H than PA1 (δ_H = 7.9 $MPa^{0.5}$), precipitates produce irregular aggregates, which is in contrast to the results obtained for individual particles. In water with the highest δ_H, the DKP moieties in PA1 tend to form hydrogen bonds much more easily with water molecules than with themselves, thereby resulting in the formation of random hydrogen bonds (Fig. 1c). As for ethanol, with the decrease in the δ_H value for the solvent, the probability of DKP–DKP interaction increases, leading to the emergence of a two-dimensional substructure (Fig. 1d). As for THF, the δ_H value for the solvent approaches PA1, which implies that the DKP moieties have a similar chance to form hydrogen bonds with the solvent and themselves, resulting in a median morphology between the network and individual particles (Fig. 1e). When solvents exhibit lower δ_H values than PA1, the DKP moieties have a greater chance to form hydrogen bonds with themselves rather than with solvent molecules, resulting in individual particles.

Mechanism of self-assembly behavior for PAs

Based on the morphological study of PA1, the formation of both hollow and cubic particles exhibits unique characteristics because they are not typical for a homopolymer without side chains. It is important and challenging to analyze this self-assembly mechanism. Polymorphism phenomenon is also reported in the self-assembly of amino acids and small peptides. The self-assembly process of these building blocks is driven by thermodynamics and kinetics, which could be easily influenced by solvent environment. For an example, diphenylalanine could self-assemble into crystal and fibrous gel, which was strongly impacted by solvents, even in a trace amount.[52,53] Similarly, regarding to the above-mentioned IR and HSP studies, hydrogen bond is considered as the dominating driving force of self-assembly, which deeply affected by poor solvents. The mechanism of the self-assembly of PA1 is shown in Fig. 4. When water is used as poor solvent, water molecules can form hydrogen bond with DKP unit, which prevents the formation of DKP–DKP hydrogen bond. Besides, water molecules also can bridge two polymer chains, as shown in Fig. 4a. As a result, PA1 particles from water show irregular gel-like morphology. When PA1 DMSO solution is added into poor solvents with low δ_H, such as acetone and toluene, polymer chains aggregate regularly due to the parallel hydrogen bond formed by DKP moieties between polymer molecules, thereby resulting in a two-dimensional sheet-like substructure (Fig. 4b). Following vigorous stirring, the sheet-like substructure eventually bends to form a hollow sphere. Because acetone has higher δ_H than toluene, polymer chains still have chance to formed hydrogen bond with acetone molecules. As a result, the packing of polymer chains from acetone is not as stable as which from toluene. Therefore, the sheet-like substructure from acetone becomes smaller, resulting in smaller hollow particles, compared to particles from toluene. Similarly, particles in Fig. 2b–e, which have been treated by acetone, are in sizes of about 1 μm. When toluene is added to the acetone droplet sample, the thermodynamic environment of the particles changes, thereby resulting in the unfolding of the sheet-like substructure. Notably, in this case, no stirring is performed. It is hypothesized that with the aid of toluene, π-stacking occurs in the benzene ring moiety of PA1 units, which also weakens the hydrogen bond between the DKP moieties because of the steric effect, resulting in the stacking of substructures and cubic morphology (Fig. 4c). When acetone is added to the cubic particles, the cubic particles decompose again to form the sheet-like substructure. Along with the relatively fast drying of acetone, the sheet-like substructures tend to bend to form hollow particles again. However, acetone dries rapidly and cannot impart sufficient bending energy as compared to that provided by vigorous stirring; therefore, the hollow particles shown in Fig. 2e are not completely formed.

Conclusion

We have established an AB-type DKP-based monomer with high solubility from a commercial dipeptide sweetener. Various DKP-based PAs, with or without other monomers, were synthesized. All the PAs showed high molecular weights and high thermal resistances. Morphologies of the homopolymer PA1 were elucidated using solvent displacement methods that employed a variety of solvents ranging from a DMSO solution to various poor solvents, thereby resulting in particles with various morphologies; for example, irregular networks as well as rugby-like and hollow particles. In particular, the preparation of hollow particles was achieved without any additive or fabrication. Furthermore, PA1 particles underwent a morphological transformation by secondary solvent treatment using the acetone and toluene dropping technique. To investigate the role of hydrogen bonds in self-assembly, IR and HSP approaches were applied to define the mechanism governing the morphology formation of DKP-based PAs. The present study provides a high potential as a self-assembly building block for functional nanomaterials.

Conflicts of interest

There are no conflicts to declare.

Acknowledgements

This work has been financially supported by Japan Science and Technology Agency (JST)-Advanced Low Carbon Technology Research and Development Program (JPMJAL10100) (ALCA), Center of Innovation (COI) program "Construction of next-generation infrastructure using innovative materials – realization of a safe and secure society that can coexist with the Earth for centuries-, Japan Society for the Promotion of Science (JSPS) of Grant-in-Aid for Scientific Research (B) (15H03864), and Cross-ministerial Strategic Innovation Promotion Program (SIP2), "Smart-bio" (Bio-oriented Technology Research Advancement Institution, NARO, Japan).

References

1 X.-Q. Dou and C.-L. Feng, *Adv. Mater.*, 2017, **29**, 1604062.
2 S. Sharma, R. Singh and S. Rana, *Int. J. BIOautom.*, 2011, **15**, 223–250.
3 B. Adhikari, C. Singh, A. Shah, A. J. Lough and H. B. Raatz, *Chem.–Eur. J.*, 2015, **21**, 11560–11572.
4 S. Basak, J. Nanda and A. Banerjee, *J. Mater. Chem.*, 2012, **22**, 11658.
5 X. Yan, P. Zhu and J. Li, *Chem. Soc. Rev.*, 2010, **39**, 1877–1890.
6 S. Mallakpour and M. Dinari, *J. Macromol. Sci., Part A: Pure Appl.Chem.*, 2011, **48**, 644–679.
7 A. Okamura, T. Hirai, M. Tanihara and T. Yamaoka, *Polymer*, 2002, **43**, 3549–3554.
8 P. Suvannasara, S. Tateyama, A. Miyasato, K. Matsumura, T. Shimoda, T. Ito, Y. Yamagata, T. Fujita, N. Takaya and T. Kaneko, *Macromolecules*, 2014, **47**, 1586–1593.
9 P. M. Fischer, *J. Pept. Sci.*, 2003, **9**, 9–35.
10 T.-J. M. Luo and G. T. R. Palmore, *J. Phys. Org. Chem.*, 2000, **13**, 870–879.
11 S. Palacin, D. N. Chin, E. E. Simanek, J. C. MacDonald, G. M. Whitesides, M. T. McBride and G. T. R. Palmore, *J. Am. Chem. Soc.*, 1997, **119**, 11807–11816.
12 A. S. M. Ressurreição, R. Delatouche, C. Gennari and U. Piarulli, *Eur. J. Org. Chem.*, 2011, 217–228.
13 S. Manchineella and T. Govindaraju, *ChemPlusChem*, 2017, **82**, 88–106.
14 A. D. Borthwick, *Chem. Rev.*, 2012, **112**, 3641–3716.
15 K. Takada, H. Yin, T. Matsui, M. A. Ali and T. Kaneko, *J. Polym. Res.*, 2017, **24**, 216.
16 K. Hanabusa, M. Matsumoto, M. Kimura, A. Kakehi and H. Shirai, *J. Colloid Interface Sci.*, 2000, **224**, 231–244.
17 K. Hanabusa and M. Suzuki, *Polym. J.*, 2014, **46**, 776–782.
18 Y. Ohta, K. Terada, T. Masuda and F. Sanda, *Heterocycles*, 2009, **78**, 1477–1483.
19 E. A. C. Davie, S. M. Mennen, Y. Xu and S. J. Miller, *Chem. Rev.*, 2007, **107**, 5759–5812.
20 K. Terada, F. Sanda and T. Masuda, *J. Macromol. Sci., Part A: Pure Appl.Chem.*, 2007, **44**, 789–794.
21 J. Akerlund, S. Harmeier, J. Pumphrey, D. C. Timm and J. I. Brand, *J. Appl. Polym. Sci.*, 2000, **78**, 2213–2218.
22 K. Terada, E. B. Berda, K. B. Wagener, F. Sanda and T. Masuda, *Macromolecules*, 2008, **41**, 6041–6046.
23 K. Terada, T. Masuda and F. Sanda, *Macromolecules*, 2009, **42**, 913–920.
24 T. Hirayama, A. Kumar, K. Takada and T. Kaneko, *ACS Omega*, 2020, **5**, 2187–2195.
25 M. Ishikawa and Y. Hashimoto, *J. Med. Chem.*, 2011, **54**, 1539–1554.
26 R. Pinal, *Org. Biomol. Chem.*, 2004, **2**, 2692.
27 E. Busseron, Y. Ruff, E. Moulin and N. Giuseppone, *Nanoscale*, 2013, **5**, 7098.
28 Y. Li, L. Yan, K. Liu, J. Wang, A. Wang, S. Bai and X. Yan, *Small*, 2016, **12**, 2575–2579.
29 D. Wang, G. Tong, R. Dong, Y. Zhou, J. Shen and X. Zhu, *Chem. Commun.*, 2014, **50**, 11994–12017.
30 G. Qing, X. Shan, W. Chen, Z. Lv, P. Xiong and T. Sun, *Angew. Chem., Int. Ed.*, 2014, **53**, 2124–2129.
31 Y. Lan, M. G. Corradini, X. Liu, T. E. May, F. Borondics, R. G. Weiss and M. A. Rogers, *Langmuir*, 2014, **30**, 14128–14142.
32 Y. Lan, M. Lv, S. Guo, P. Nasr, V. Ladizhansky, R. Vaz, M. G. Corradini, T. Hou, S. M. Ghazani, A. Marnangoni and M. A. Rogers, *Soft Matter*, 2019, **15**, 9205–9214.
33 F. Stegink, *Aspartame: physiology and biochemistry*, CRC Press, 1984, vol. 12.
34 G. Lindeberg, *J. Chem. Educ.*, 1987, **64**, 1062.
35 J. D. Berset and N. Ochsenbein, *Chemosphere*, 2012, **88**, 563–569.
36 S. M. Gaines and L. B. Jeffrey, *J. Org. Chem.*, 1988, **53**, 2757–2764.
37 R. M. Lynden-Bell and J. C. Rasaiah, *J. Chem. Phys.*, 1997, **107**, 1981–1991.
38 A. W. Omta, M. F. Kropman, S. Woutersen and H. J. Bakker, *Science*, 2003, **301**, 347–349.
39 G. Perego, G. D. Cella and C. Bastioli, *J. Appl. Polym. Sci.*, 1996, **59**, 37–43.
40 S. Zanganeh, A. Kajbafvala, N. Zanganeh, M. S. Mohajerani, A. Lak, M. R. Bayati, H. R. Zargar and S. K. Sadrnezhaad, *Appl. Phys. A: Mater. Sci. Process.*, 2010, **99**, 317–321.
41 R. A. Ramli, *RSC Adv.*, 2017, **7**, 52632–52650.
42 T. Zhang, C. Jin, L. Wang and Q. Yin, *RSC Adv.*, 2014, **4**, 36882–36889.
43 Y. Cao, B. You and L. Wu, *Langmuir*, 2010, **26**, 6115–6118.
44 J. Han, G. Song and R. Guo, *Adv. Mater.*, 2006, **18**, 3140–3144.
45 T. Kaneko, M. Higashi, M. Matsusaki, T. Akagi and M. Akashi, *Chem. Mater.*, 2005, **17**, 2484–2486.
46 B. H. Hong, J. Y. Lee, C.-W. Lee, J. C. Kim, S. C. Bae and K. S. Kim, *J. Am. Chem. Soc.*, 2001, **123**, 10748–10749.
47 M. R. Molla and S. Ghosh, *Chem. Mater.*, 2011, **23**, 95–105.
48 Y. Yin, Z. Gao, Y. Bao, B. Hou, H. Hao, D. Liu and Y. Wang, *Ind. Eng. Chem. Res.*, 2014, **53**, 1286–1292.
49 C. Panayiotou, *Phys. Chem. Chem. Phys.*, 2012, **14**, 3882–3908.
50 S. Abbott, C. M. Hansen and H. Yamamoto, *Hansen solubility parameters in practice complete with eBook, software and data*, 2013.
51 C. M. Hansen, *Hansen solubility parameters: a User's Handbook*, 2011, vol. 118.
52 J. Wang, K. Liu, X. Ruirui and X. Yan, *Chem. Soc. Rev.*, 2016, **45**, 5589–5604.
53 J. Wang, K. Liu, L. Yan, A. Wang, S. Bai and X. Yan, *ACS Nano*, 2016, **10**, 2138–2143.